1987

Steady flow field measurements using Laser Doppler Velocimetry.

Wilson, Ricky E.; Bodapati, Satyanarayana.

NAVAL POSTGRADUATE SCHOOL
Monterey, California

THESIS

STEADY FLOW FIELD MEASUREMENTS
USING
LASER DOPPLER VELOCIMETRY

by

Ricky E. Wilson

December 1987

Thesis Advisor Satya Bodapati

REPORT DOCUMENTATION PAGE

1a REPORT SECURITY CLASSIFICATION UNCLASSIFIED	1b RESTRICTIVE MARKINGS
2a. SECURITY CLASSIFICATION AUTHORITY	3 DISTRIBUTION/AVAILABILITY OF REPORT Approved for public release; distribution unlimited
2b DECLASSIFICATION / DOWNGRADING SCHEDULE	
4 PERFORMING ORGANIZATION REPORT NUMBER(S)	5 MONITORING ORGANIZATION REPORT NUMBER(S)
6a NAME OF PERFORMING ORGANIZATION Naval Postgraduate School — 6b OFFICE SYMBOL (If applicable) 67	7a NAME OF MONITORING ORGANIZATION Naval Postgraduate School
6c. ADDRESS (City, State, and ZIP Code) Monterey, California 93943-5000	7b. ADDRESS (City, State, and ZIP Code) Monterey, California 93943-5000
8a. NAME OF FUNDING/SPONSORING ORGANIZATION — 8b OFFICE SYMBOL (If applicable)	9. PROCUREMENT INSTRUMENT IDENTIFICATION NUMBER
8c. ADDRESS (City, State, and ZIP Code)	10 SOURCE OF FUNDING NUMBERS PROGRAM ELEMENT NO. / PROJECT NO. / TASK NO / WORK UNIT ACCESSION NO

11 TITLE (Include Security Classification)
STEADY FLOW FIELD MEASUREMENTS USING LASER DOPPLER VELOCIMETRY

12. PERSONAL AUTHOR(S)
Wilson, Ricky E.

13a TYPE OF REPORT	13b TIME COVERED	14 DATE OF REPORT (Year, Month, Day)	15 PAGE COUNT
Master's Thesis	FROM ______ TO ______	1987 December	52

16. SUPPLEMENTARY NOTATION

17 COSATI CODES			18 SUBJECT TERMS (Continue on reverse if necessary and identify by block number)
FIELD	GROUP	SUB-GROUP	LDV, Laser Doppler Velocimetry

19 ABSTRACT (Continue on reverse if necessary and identify by block number)

A computer-integrated LDV system utilizing a Helium-Neon laser was designed, assembled and tested for use in the study of steady flow field quantities. All system elements were integrated to include a traverse mechanism, signal processing and conditioning, computer interface and display.

The system was initially calibrated utilizing a rotating wheel of known velocity. Experimental flow measurement tests of the system were conducted across a conventional free jet flow and in the Naval Postgraduate School low speed wind tunnel. The flow field velocity measurements made in the wind tunnel were verified using an existing pressure data acquisition station and a standard pitot static probe.

20 DISTRIBUTION/AVAILABILITY OF ABSTRACT ☒ UNCLASSIFIED/UNLIMITED ☐ SAME AS RPT ☐ DTIC USERS	21 ABSTRACT SECURITY CLASSIFICATION UNCLASSIFIED	
22a NAME OF RESPONSIBLE INDIVIDUAL Professor Satyanarayana Bodapati	22b TELEPHONE (Include Area Code) (415) 694-4144	22c OFFICE SYMBOL 67Bu

DD FORM 1473, 84 MAR — 83 APR edition may be used until exhausted. All other editions are obsolete

SECURITY CLASSIFICATION OF THIS PAGE

☆ U.S. Government Printing Office 1986—606-24.

19. The system was found to be adequte for advanced classroom instruction in LDV measurements. Upgrading to an Argon-Ion laser would be required to achieve the higher signal levels needed to measure turbulence quanties.

Approved for public release; distribution is unlimited.

Steady Flow Field Measurements Using Laser Doppler Velocimetry

by

Ricky E. Wilson
Lieutenant, United States Navy
B.S., United States Naval Academy, 1980

Submitted in partial fulfillment of the
requirements for the degree of

MASTER OF SCIENCE IN AERONAUTICAL ENGINEERING

from the

NAVAL POSTGRADUATE SCHOOL
December 1987

C-1

ABSTRACT

A computer-integrated LDV system utilizing a Helium-Neon laser was designed, assembled and tested for use in the study of steady flow field quantities. All system elements were integrated to include a traverse mechanism, signal processing and conditioning, computer interface and display.

The system was initially calibrated utilizing a rotating wheel of known velocity. Experimental flow measurement tests of the system were conducted across a conventional free jet flow and in the Naval Postgraduate School low speed wind tunnel. The flow field velocity measurements made in the wind tunnel were verified using an existing pressure data acquisition station and a standard pitot static probe.

The system was found to be adequate for advanced classroom instruction in LDV measurements. Upgrading to an Argon-Ion laser would be required to achieve the higher signal levels needed to measure turbulence quantities.

TABLE OF CONTENTS

I. INTRODUCTION 7

II. THEORY AND DESIGN CONFIGURATIONS 8
- A. LASER DOPPLER VELOCIMETRY 8
- B. SYSTEM DESIGN CONSIDERATIONS 11
  - 1. LDV Classification 12
  - 2. Laser types 12
  - 3. Collection Methods 13
  - 4. Particle Seeding 14

III. INSTRUMENTATION 16
- A. LDV INTEGRATED OPTICS 16
- B. FORWARD TRANSMITTED BEAM PATH 16
- C. SCATTERED LIGHT PATH 24
- D. SIGNAL FLOW AND PROCESSING 28
- E. COMPUTER INTERFACE 33
- F. EQUIPMENT SET UP 35

IV. DATA ACQUISITION 39
- A. COMPUTER SOFTWARE 39
- B. CALIBRATION PROCEDURE 39
- C. FREE JET 40
- D. WIND TUNNEL DATA 40

V. RESULTS AND DISCUSSION 42
- A. CALIBRATION RESULTS 42
- B. FREE JET PROFILE 43
- C. WIND TUNNEL MEASUREMENTS 46

VI. CONCLUSIONS AND RECOMMENDATIONS 47

LIST OF REFERENCES 49

INITIAL DISTRIBUTION LIST 50

ACKNOWLEDGEMENTS

This thesis project was partially supported by Naval Air Systems Command as part of a larger project for future thesis students in the research of aircraft Super-maneuverability. The project was conducted at the Naval Post Graduate School as part of the Navy-NASA Joint Institute of Aeronautics.

I would like to thank my thesis advisor Professor Satyanarayana Bodpati and also Dr. M.S. Chandrasekhara of the Joint Institute for their guidance and patience throughout the course of this project. I would also like to express my sincere gratitude to them for having allowed me the opportunity to learn about and work with Laser Doppler Velocimetry.

I would also like to give special thanks to Jack King whose good humor, as much as his multifaceted technical talents made the work that much easier. Also a special thank you to Chet Heard for his expert help at a crucial moment.

Finally I would like to take this opportunity to express my appreciation for the support and encouragement of my wife Terry and my daughter Audrey, for without them it would not have been possible.

I. INTRODUCTION

The basic goal of this thesis project was to design, assemble and validate a computer integrated single component Laser Doppler Velocimetry system which would be suitable for use in steady flow field measurements.

The system was to be utilized in the NPS low speed wind tunnel for advanced classroom laboratory instruction in LDV measurement techniques. A traverse system with positional read out was determined necessary in order to adequate determine the eam crossing position. Additionally the total system was required to be easily adaptable to permit future use in the research of dynamic stall.

A three step procedure was followed to verify system reliability. First the completed system was calibrated by measuring the velocity at a specific radius on a wheel rotating at a known velocity. Measurements were then made in a low velocity free jet to obtain a velocity profile plot and ascertain system usability in an actual flow field environment. Finally measurements were made in the NPS low speed wind tunnel and compared with velocities obtained using a standard pitot static system.

II. THEORY AND DESIGN CONFIGURATIONS

A. LASER DOPPLER VELOCIMETRY

The physical principles of Laser Doppler Velocimetry are simple in that the physical characteristics of the individual laser beams and the geometry of a dual beam crossing can be used to precisely determine the velocity components of a flow field. Using the well known doppler effect.

In a dual beam system two collimated and coherent light beams are focused at the same point in space creating what is referred to as the probe volume. The volume is elliptical in shape and Gaussian in its intensity distribution due to the physical characteristics of the beams. Figure 1 illustrates the physical construction of the probe volume.

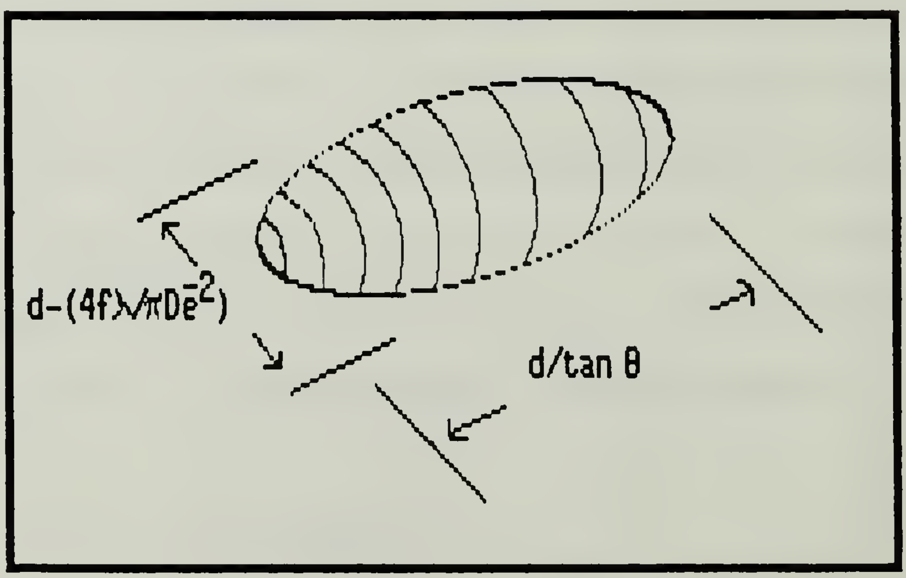

Figure 1 Probe Volume Geometry

As a result of the constructive and destructive interference of the wave fronts of the two beams a fringe pattern is created. Figure 2 illustrates the fringe pattern which is termed the "interference fringe" model [Ref 1 p. 110]. The heavy lines in the figure are the resultant planes of constructive interference. The spacing between the planes is determined geometrically to be :

$d = \lambda/2 \sin\theta$ Equation 1

Where lambda is the wavelength of the light. In actual practice:

$\theta = \tan^{-1}$ [1/2 beam spacing /focal length of lens]

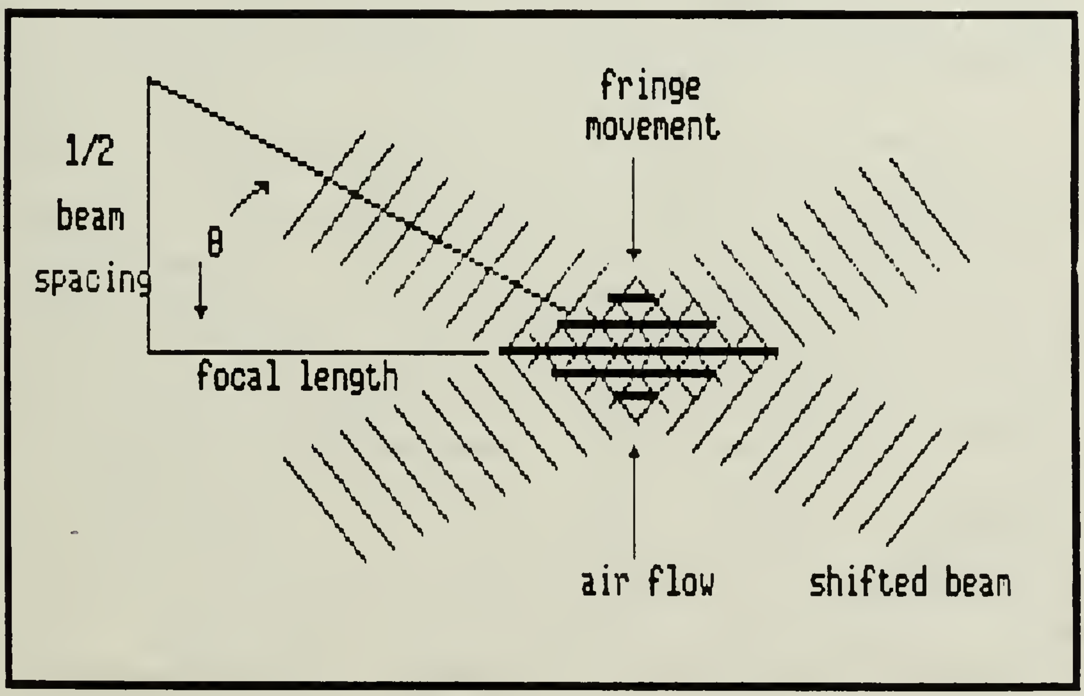

Figure 2 Fringe Model

As a particle passes through the volume the scattered light is doppler shifted, the frequency of which is the velocity signal. The velocity of the particle can be determined by using the relation.

$$V_{seed} = f_{doppler} \times d_f \qquad \text{Equation 2}$$

Where $f_{doppler}$ equals the signal frequency and d_f equals the fringe spacing. The flow velocity is inferred from this velocity since the particle is assumed to be traveling with the flow. It should be noted that the velocity that is measured is perpendicular to the fringe plane which results in a 180 degree ambiguity for the resolved direction of flow.

When a frequency shift is introduced into one of the two beams, the fringes will move at a frequency which is equal to the frequency of the shift employed. Such a shift is introduced by and acousto-optic device called a Bragg cell. Figure 2 illustrates the orientation of the resulting fringe movement in such a case. Referring to equation 1 the formula for frequency now becomes:

$$f_{signal} = f_{shift} \pm f_{doppler} \qquad \text{Equation 3}$$

In equation 3 if the particle is moving in the opposite direction of the fringe movement, the frequency of the signal produced will be the frequency of the doppler plus the frequency of the shift. Therefore if the particle moves with the fringes the sign in equation 3 is negative.

In resolving the directional ambiguity the velocity equation now becomes.

$V_{seed} = \{\lambda 2\sin(\theta/2)\}*(f_{signal} - f_{eff})$ Equation 4

Where f_{eff} is the effective frequency employed. The four equations developed are utilized by the operator or by the software developed for the computer in determining the flow velocity.

B. SYSTEM DESIGN CONSIDERATIONS

Laser Doppler Velocimetry has become recognized as the definitive optical technique for obtaining fluid flow velocities. The method is advantageous in comparison to non-optical techniques such as hot wires or pitot static probes primarily because it is non-intrusive and once established requires no calibration.

Some of the restrictive aspects of Laser Doppler Velocimetry emerge in the initial setup and alignment of the required optics. The alignment process is tedious but must be precise in order to achieve meaningful results and avoid complications later on. Additionally it is essential that the laser have optical access to the test flow being measured. Generally the flow will also require some form of particle seeding apparatus to make the measurements. Finally the signal conditioning and processing techniques are crucial and need to be performed properly to avoid serious measurement errors.

1. LDV Classification

The classification of an LDV system is determined by how many components of velocity one can measure with the system at one time, how many beams are used in this measurement and how the particle scattered light is collected.

There are numerous configurations of LDV systems which have been developed for specific uses in various flow field environments. The technique which is used most often is the dual beam system [Ref 2 p. 52]. In this system the originating laser beam is split into two beams of equal power and intensity. These two beams are focussed by a lens to create the probe volume and the resulting fringe pattern as discussed earlier. The light scattered by the particle is collected by a set of receiving optics, converted to an electric voltage by a photodetector and then amplified and conditioned by signal processing equipment. The output from these can be interfaced with a computer to provide optimal data reduction and presentation.

2. Laser types

Two types of lasers are commonly used in LDV's: the Helium-Neon and the Argon-Ion laser. The choice of the laser and its power in any specific LDV system is dependent upon the characteristics of the flow, and the dimensions of the experimental set up, in addition to the number of components of velocity measured.

The Helium-neon laser is relatively inexpensive, simple to use and very reliable. For this reason this type of laser was chosen to initially establish the system and ease the trouble shooting problem.

3. Collection Methods

Scattered light collection methods for both the single component and multiple component LDV's are of two basic types, forward scatter and back scatter collection.

In the forward scatter system the Doppler shifted light is collected forward of the transmitted beam. In the backscatter collection method the shifted light is collected via the same path in which the original beams were transmitted.

One of the problems associated with the forward collection method is that it requires optical access on both side of the test section. It also requires that dual traverse mechanisms, which connect the receiving and transmitting optics be synchronized. An additional restriction for this project was to avoid interference with currently installed positioning equipment on the wind tunnel.

For the above reasons the backscatter collection method was chosen for this project. The major disadvantage of collecting the light in this manner is that the signal strength is about two orders of magnitude less than in the forward scatter mode and therefore usually requires a higher power level to alleviate some of the inherent signal loss.

4. Particle Seeding

The quality of the signal received in LDV depends on the ability of a particle passing through the probe volume to scatter light. The particles may be naturally present or introduced in the flow by a seeder. Naturally present particles, if the right size, are too small in number (in air) to yield sufficient signal. And thus generally a particle seeder is almost always needed. The effect of particle seeding is to increase the data rate (number of validated measurements per second) and effectively increase the signal to noise ratio. Excessive seeding would simply decrease the signal to noise ratio by increasing the phase noise in the signal. Typically particles on the order of 1 micron are used to seed the flow. Particles of this size can follow rapid fluctuations in the flow up to 1khz [Ref 2 p. 303]. Particles larger than this generally do not follow the flow and particles smaller than this usually cause a large level of background noise. Thus, careful control of the seed size is important for accurate and reliable measurements. This requires the use of some form of particle generator, that generates the required size of particles at a specified rate. The seeding arrangement developed for this system is discussed in detail in chapter two section F.

III. INSTRUMENTATION

A. LDV INTEGRATED OPTICS

The system chosen for use at the Naval Postgraduate school was designed and supplied by DANTEC electronics. The 55X LDA modular optics is an integral optic system which can be configured to operate in a multitude of modes by changing individual system components. The system optics are compatible with both the Helium-neon and the Argon-ion lasers.

For purposes of initial optical alignment and testing, the system was configured in the dual beam single component backscatter mode utilizing a Spectra-Physics Model 124B Helium-Neon 15mw laser.

B. FORWARD TRANSMITTED BEAM PATH

The forward beam path through the modular optics is as illustrated in Figure 3. Each component is labeled as it is discussed in the following paragraphs.

The first group of components are polarization rotators also referred to as retarders or wave plates. The first quarter wave plate is attached to the exit port of the laser and causes the beam to be polarized in a circular manner. The rotator accomplishes this by a phenomena known as Birefringence. The beam is then passed through a second

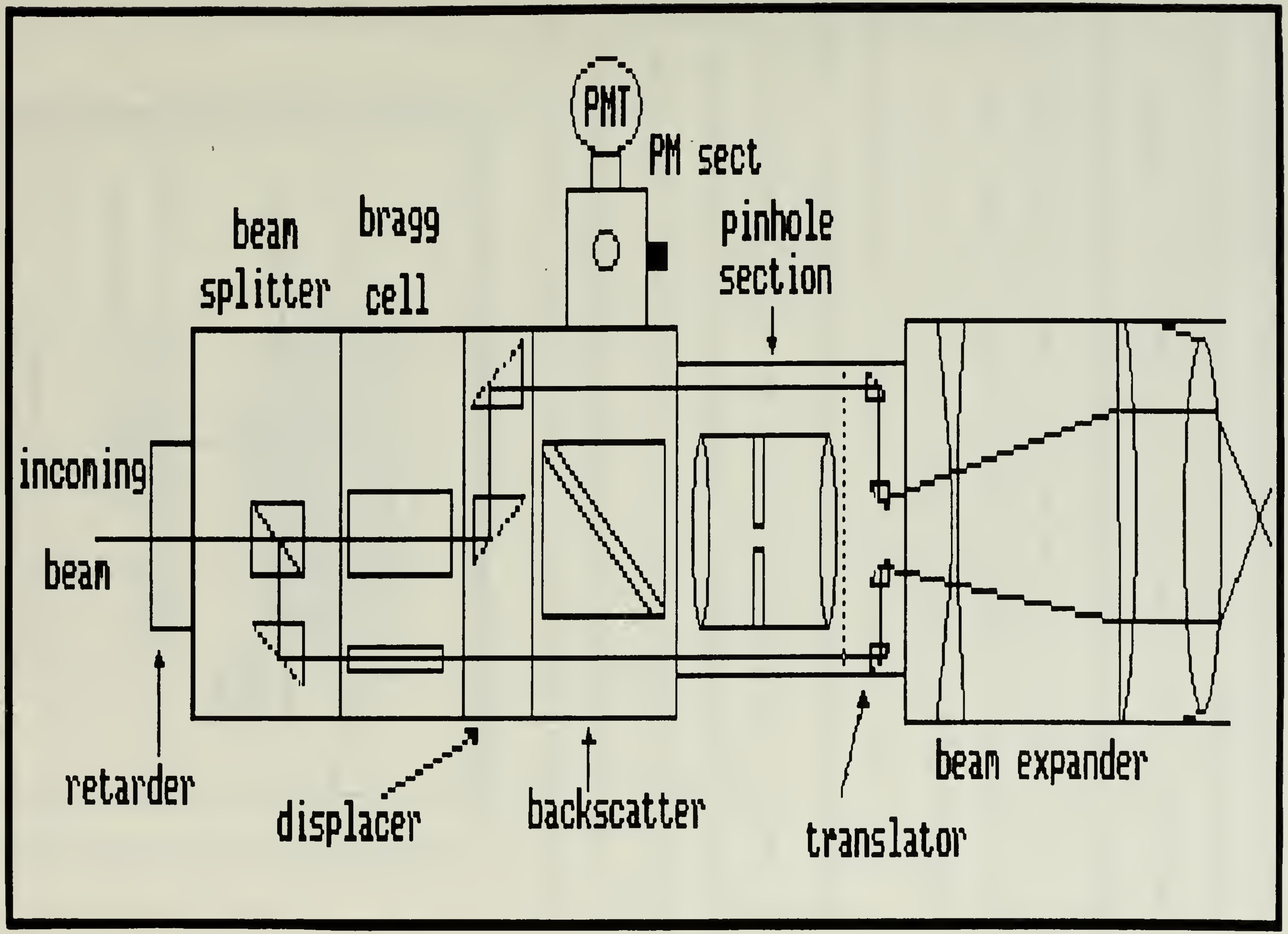

Figure 3 Forward Beam Path

quarter wave plate mounted on the rear of the integral optics system. The polarization can be adjusted to a specific angle by rotating the plate mounting ring. For a beam to be optimally transmitted through the beamsplitter or prisms the beam polarization must be perpendicular to the plane defined by the incident and refracted or reflected beam.

The beam then enters a color neutral beam splitter where it is split into two beams of equal power and intensity. The split beam is displaced 30mm off the central axis but remains parallel with the original beam. The beam splitter consists of two prisms which have a thin film coating on the faces joining them (see Figure 4). The coating permits an equal division of power between the

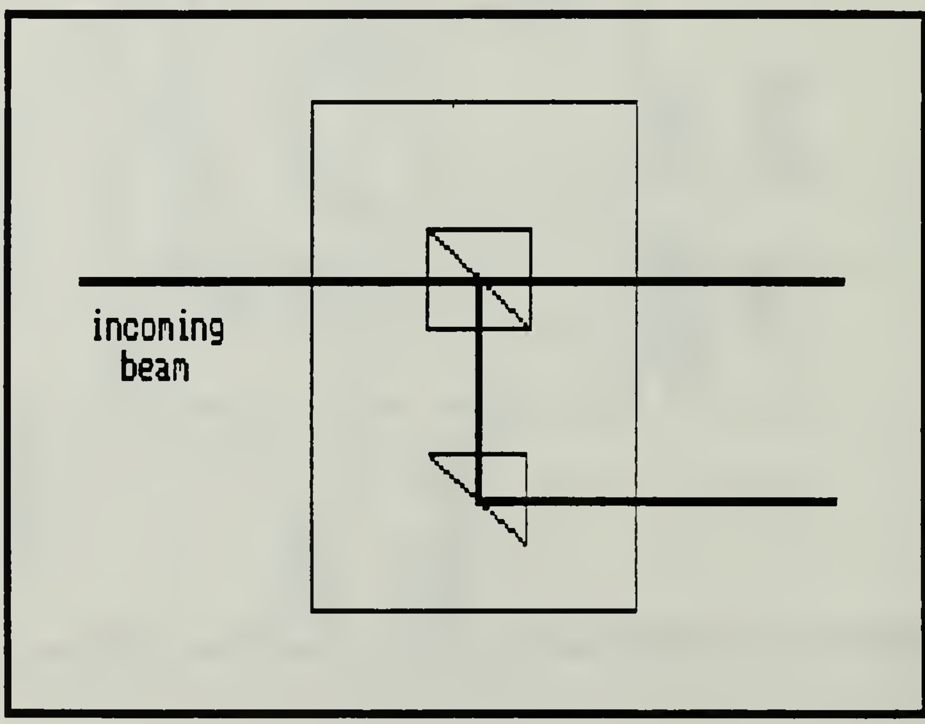

Figure 4 Beam Splitter

split beams. The second solitary glass prism with the single 45 degree surface reflects the beam internally at the glass air interface to translate the beam as illustrated. These two prisms are used repeatedly throughout the system in different components.

The original undeflected beam is then passed through the bragg cell shown in Figure 5. The primary function of this component is to induce the frequency shift in a single beam for the reasons discussed earlier. The beam displaced by the triangular prism is passed through a glass rod in order to keep the optical path lengths of the individual beams equal. The bragg cell in this system is constructed using a glass cell, an acoustic absorber and a transducer. The transducer imparts a frequency to the glass cell which

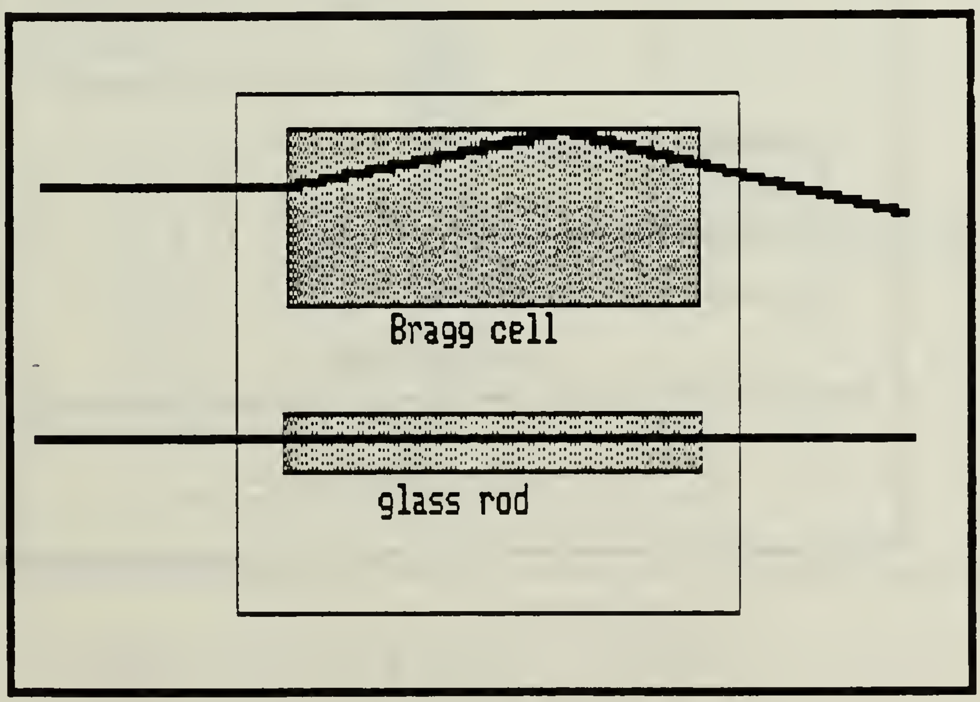

Figure 5 Bragg Cell Unit

in turn acoustically transmits this frequency to the incoming beam by setting up a standing wave pattern in the cell. At this point the beam enters the beam displacer unit (see Figure 6). This unit only affects the shifted beam. It has two basic purposes 1) it corrects the shifted beam back parallel with the unshifted beam and 2) it displaces the shifted beam 30mm off axis. This results in a total beam separation of 60 mm. This separation aligns the beams with the transmission holes in the remaining components. The beam passes through the backscatter and the pinhole sections unaltered. These components realize their function in the backscatter collection process.

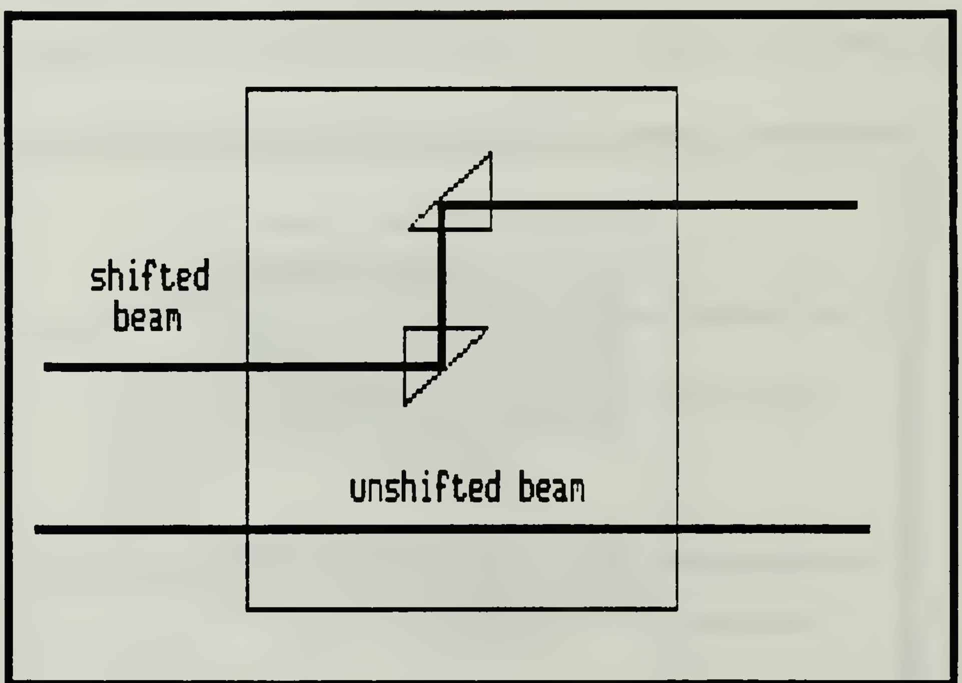

Figure 6 Beam Displacer Unit

The beam translator section (see Figure 7) consists of the same triangular prisms as used in previous sections. This section allows the user to select the separat on distance of the outgoing beams. This permits the control of the number of fringes in the probe volume and thereby optimize the number of fringes for a given measuring condition. The number of fringes can by calculated by the following formula:

$$N_f \sim D/d$$

Where d is the beam diameter and D is the beam spacing set by the beam translator. More importantly the beam separation can be brought down to within the range needed

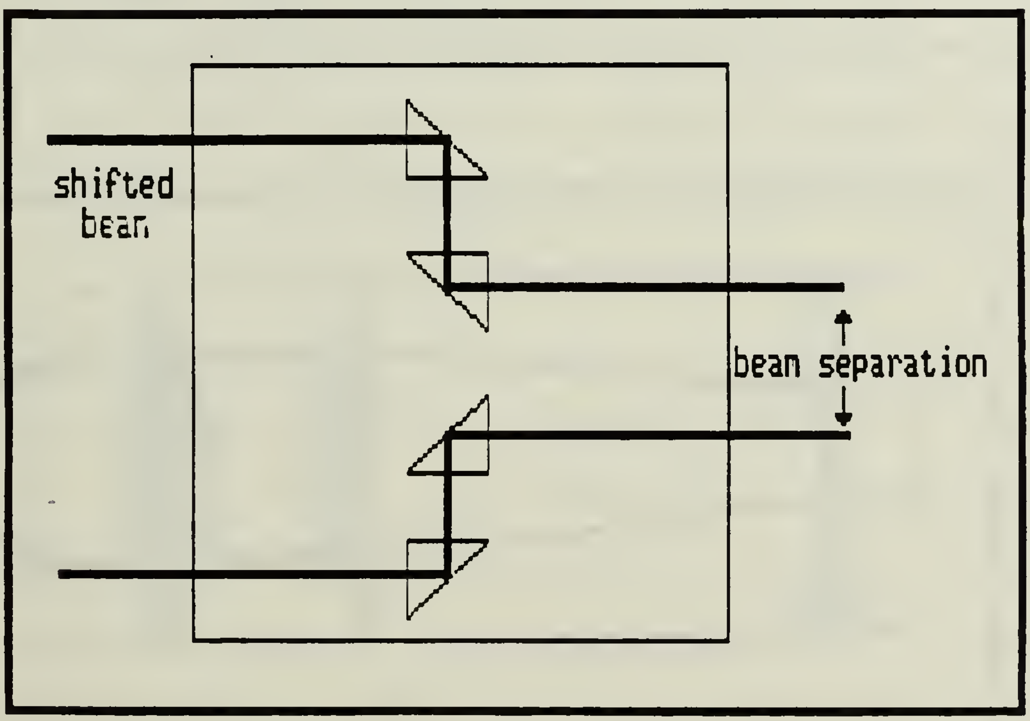

Figure 7 Beam Translator

if a beam expander is used further along the optic axis. A related formula directly equates the seed particle size to the optimal beam separation.

$$\sin \theta = \lambda 2/rp$$

Where rp is the radius of the seed particle in microns [Ref 2 p. 332]. If the particle size is unknown the beam separation can be adjusted to provide the maximum signal to noise ratio by using the translator.

The beam is then passed through a beam expander section which reduces the beam waist radius by increasing the diameter (D) of the incident beam. The expander is composed of two primary lenses, one lens of a short focal length and a second of long focal length. Figure 8 illustrates the construction of this component.

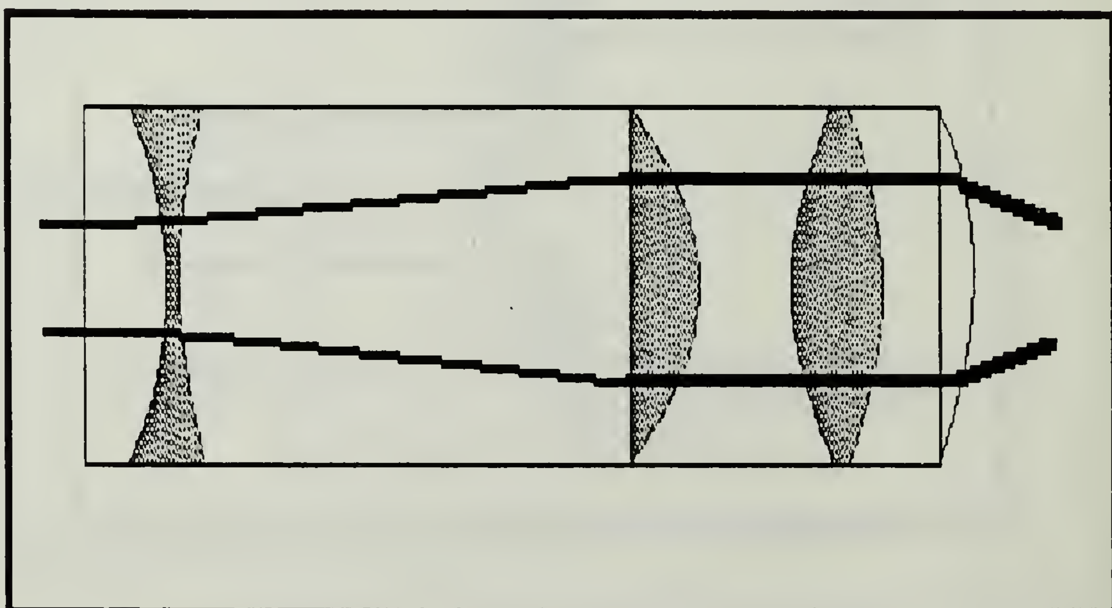

Figure 8 Beam Expander

The magnification of the beam diameter is a direct function of the ratio of the focal length of the two primary lenses. For this expander the expansion factor is 1.9. This diminishes the probe volume cross section by the same factor. It also increases the light intensity collected by a factor of about 14 which in effect increases the signal to noise ratio by a factor of 7.

Attached to the end of the beam expander section is the primary objective lens which focuses the beam at the desired point. This lens is interchangeable and can be substituted with lenses of different focal lengths to meet the probe volume positioning requirements of different measuring situations. The ideal lens for any optical system would be a non-spherical or Aspheric lens. This type of lens does not have the optical losses associated with the spherical lenses but is extremely costly to produce. For this reason this system uses the spherical lenses.

When collimated light is passed through a spherical lens the light focuses at different points in space depending upon the radius at which the light enters the lens. This is referred to as spherical aberration and is a function of the lens geometry. Another problem associated with these lenses is Chromatic (or color) aberration. This occurs when light with different wavelengths is focused at different points caused by differences in refraction of the light through the lens.

In order to correct for chromatic aberration the lenses used in this system are constructed of two materials of different chromatic dispersions which when sealed to form a single lens compensate the reflective qualities of the lens. This also helps to correct for some of the spherical aberration as well.

C. SCATTERED LIGHT PATH

At this point the backscatter light is collected via the path shown in Figure 9. The scattered light is received through the same primary objective lens and beam expander section as in the forward beam path.

The first dedicated backscatter component is the pinhole section shown in Figure 10. This section consists of two 48mm diameter achromatic lenses. Both lenses have their focal points located at the center pinhole. The light received from the expander section, which includes the background light (noise) in addition to the Doppler information is focused via the first lens at the pinhole. The pinhole acts as a spatial filter and blocks out a large portion of the extraneous light. The second lens focuses this light on the backscatter section.

The backscatter section contains an aluminum quartz plated mirror which reflects the collected light with an

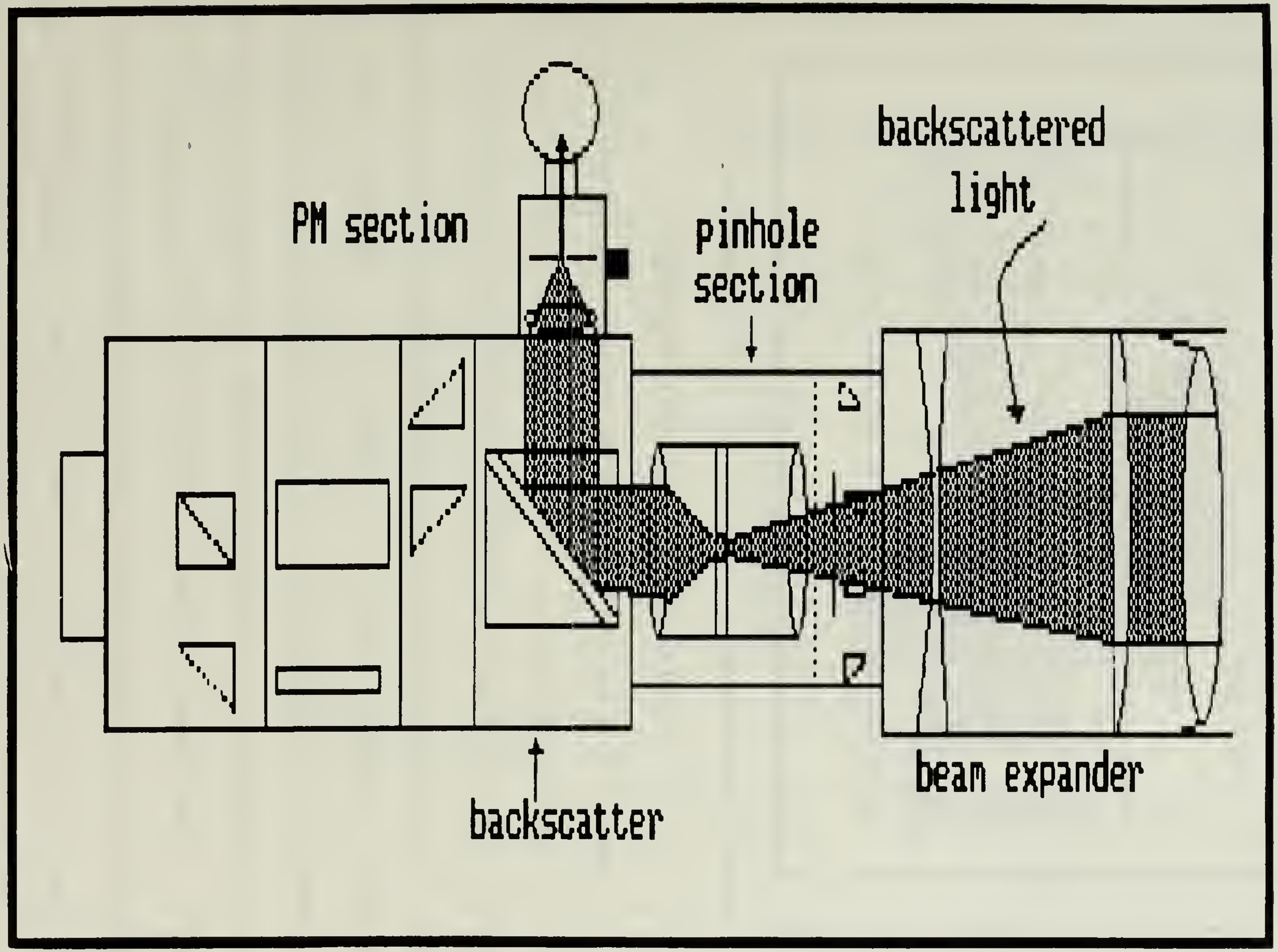

Figure 9 Scattered Light Path

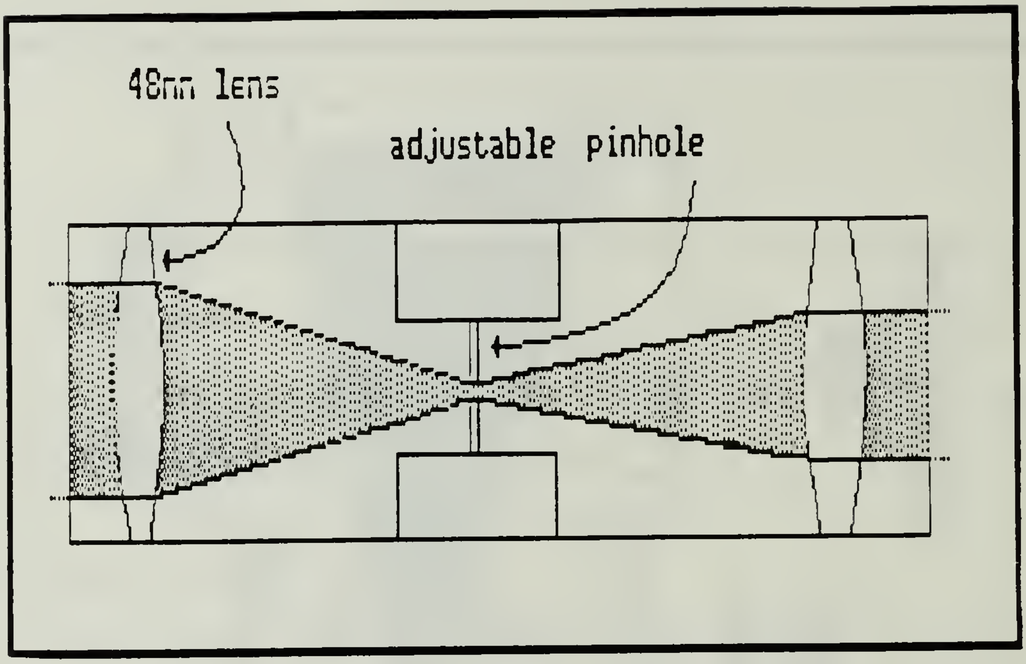

Figure 10 Pinhole Section

efficiency of greater than 90% into the photo multiplier section (see Figure 11).

The PM section consists of a series of lenses which focus the incoming beam on another pinhole which serves as a second spatial filter. Also contained within the PM section is a line filter. A line filter is a color filter which is centered on the 632.8 nm wavelength of the He-Ne laser. Its function is to filter all frequencies of light other than the 632.8nm light which contains the Doppler frequency information. The desired signal is slightly attenuated but the other frequencies are almost completely removed via the destructive interference. The PM section also contains an magnifying glass which allows the user to view the probe volume and center the incoming scattered

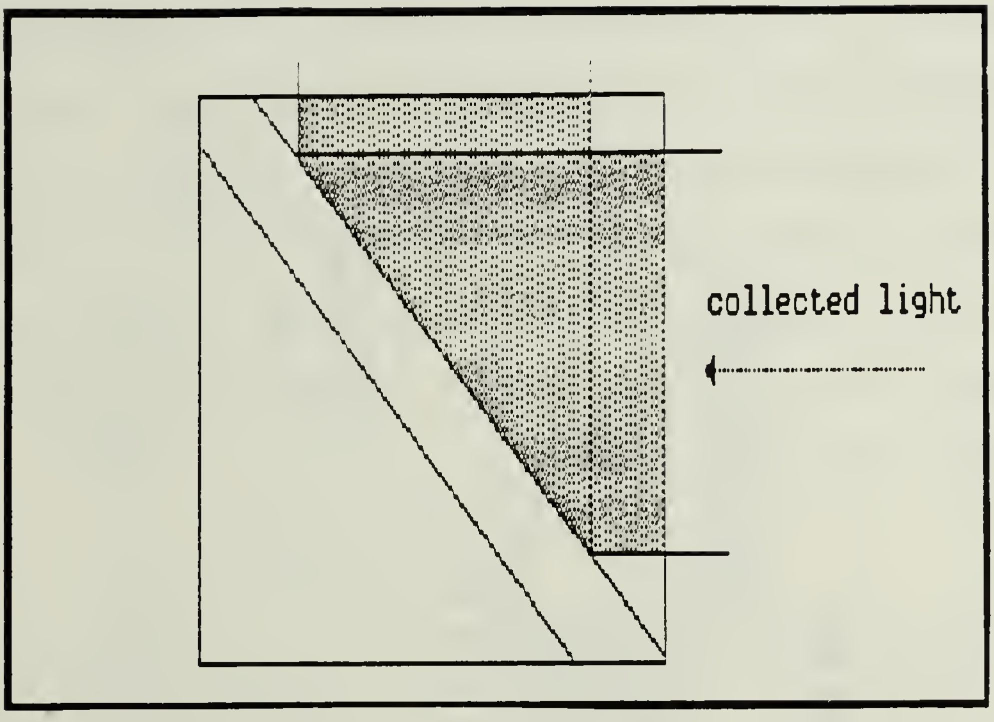

Figure 11 Backscatter Section

light through a second spatial filter and into the Photo Multiplier Tube (PMT).

The PMT consists of a cathode, anode and a series of dynodes. When light falls on the photo cathode, it results in the emission of photons. The dynode acts as the amplifier of the PMT replicating numerous electrons for each one received. Several dynodes are placed in series resulting in total amplifications of the order of 10^7. This avoids excessive transmission losses and reduces the requirement for large amplification of the signal by the processing equipment which would result in a severe distortion of the signal. The signal is then received at the anode where it is transmitted to the signal processing equipment. The PMT has a typical operating voltage of 1250 volts with a maximum of 2000 volts. It also provides for excellent low frequency response and allows high gain, and variable gain control with low noise introduction.

Although not an integral part of the laser optics, the windows through which the beams must pass in order to enter the flow plays an important role in the total system effectiveness. It is important to have clean windows to reduce the signal losses.

D. SIGNAL FLOW AND PROCESSING

The Dantec signal processing system is consists of two basic components. The 55N10 frequency mixer and the 55L90a LDA counter processor.

The counter processor is a composite component made up of several modules. These modules in addition to the fringe counters include the high voltage control for the PMT, an attenuator , a band pass filter, a threshold control, a comparator unit, and a data rate module. Figure 12 is a diagram of the signal flow through these components.

The high voltage power supply module controls the input voltage supply to the PMT and thereby controls the strength of the output signal.

From the PMT the signal is passed to the frequency mixer where the resultant frequency can be up or down mixed

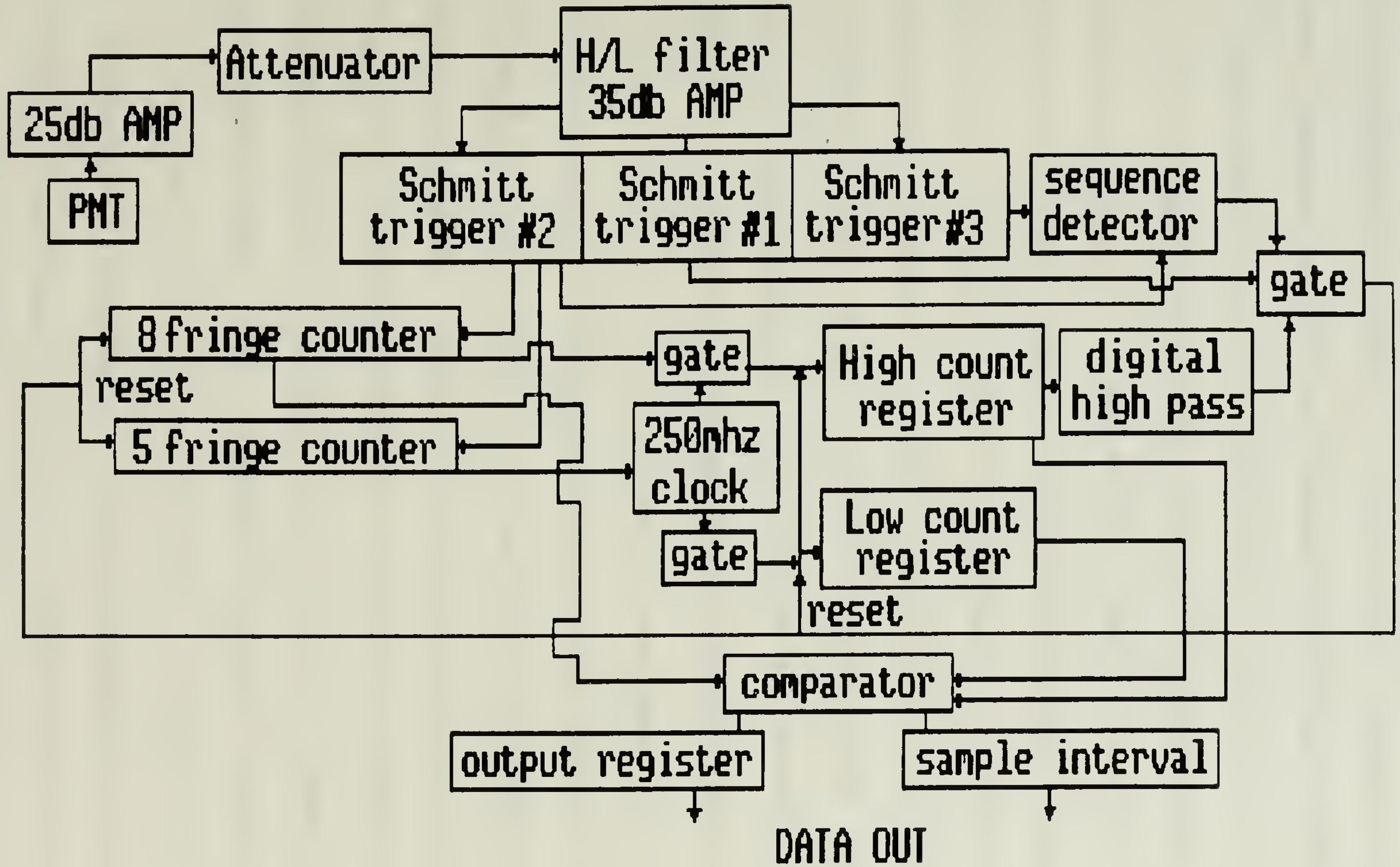

Figure 12 Signal Flow Diagram

in the selectible range from 10 khz to 9mhz. The resultant frequency output from this component is connected to the frequency counter where it is first preamplified 25db. From here the signal is passed to the attenuator which can be set to attenuate the signal from 0 to -31db. This reduces any effects of over amplification by the PMT in case of a strong signal. The signal is then amplified 35db and filtered. The high pass filter can be selected at 1,4,16,64 and 256 Khz or at 1,4,6 Mhz. This in effect removes the low frequency pedestal signal resulting from the Gaussian distribution of the beam. The signal is then low pass filtered with settings at 256khz or at 1,4,16 or 100mhz. This removes any high frequencies associated with multiple small particle crossings.

At this point the filtered signal is passed to Schmitt trigger #2 which initiates a sequence of logical pulses corresponding to the frequency of the combined signal, if the signal first exceeds a 200mv input level and then crosses through zero. At this point the doppler burst has become a purely digital signal and the 55L90a counter module is activated.

The purely digital signal is passed to the 5 fringe counter and the 8 fringe counter. When the signal reaches these counters two gates are opened which allow a series of 250mhz clock pulses to accumulate in the high count and low count registers. After 5 fringe counts gate 1 closes. The number of counts contained in the low count register can be represented by Cl. Similarly gate 2 closes after 8 fringe counts and Ch corresponds to the counts in the high count register.

The comparator computes the comparative accuracy by using the equation 100 x [Ch - 8/5 * Cl] <= e. Where 'e' is the operator desired validation accuracy as selected from 1.5 to 12% or off which removes the comparator from the circuitry.

Spurious signals can be processed by the counter if left in this configuration. For example in the case of multiple particle crossings where the time between crossings would correspond to a continuation of the normal doppler signal. To avoid this occurrence a second Schmitt trigger #3 with a level set at 100mv is incorporated in the counter. Output from both Schmitt triggers are input to a sequence detector which resets the counters if a 100mv crossing is not followed by a 200mv crossing. This in effect detects any spaces between multiple particle crossings and resets the counter.

The threshold window is controlled by Schmitt trigger #1 which initiates at a specified level above 200mv as selected by the threshold settings from 1 to 20db. This essentially acts as a large particle rejecter removing bursts which do not fall within the threshold window and resetting the counters, thereby, limiting frequency counts to those particles which are assumed to be following the flow.

A digital high pass is incorporated to insure that no frequencies are output from the counter which are below the setting on the high pass filter. If a spurious signal does occur it resets the counters.

The 8 fringe counter initiates the comparator and outputs a compare signal to the data rate module. The comparator also outputs a data ready signal to the data rate module.

The data rate module can be selected to display the data rate in Hz or in Khz as a function of the compare signals or, percent of validation as a function of the comparator equation. Validations of less than 500 with the 1.5% setting are the result of a poor doppler signal.

Data is accumulated in the output register and the sample interval registers and output as two 12 bit words. One word of doppler data from the output register and one word of time data in the sample interval register. The time data represents the elapsed time between validated signals from the comparator.

This information is passed to the buffer which facilitates computer interfacing.

E. COMPUTER INTERFACE

The Dantec 57G20 buffer consists of the 57G120 input multiplexer the 57G106 control logic board, the 57G170 output demultiplexer board, the 57G127 output logic buffer, and the 56G169 IEEE interface board. In order to permit eventual expansion to measure additional velocity components a 57G149 coincidence filter is also installed. The function of the coincidence filter is to control the timing of the input data received from two counters.

The binary coded data as received from the counter processor is handled as illustrated in Figure 13. In the input path the data is received and stored by the input multiplexer which provides for 8 to 1 multiplexing with four channels available. The output from this board is in a 16 bit word format. The word consist of 3 bit address, 12 bits data and 1 bit zeroed (not used).

The output is controlled by the control logic board. The information is read out to an 8k buffer in the output logic board via the IEEE interface board. The IEEE interface board converts raw data and address information from the buffer interface to the standard IEEE format utilized by the computer GPIB board.

The Dantec computer software requests to the buffer are controlled via the GPIB interface board through device address 10.

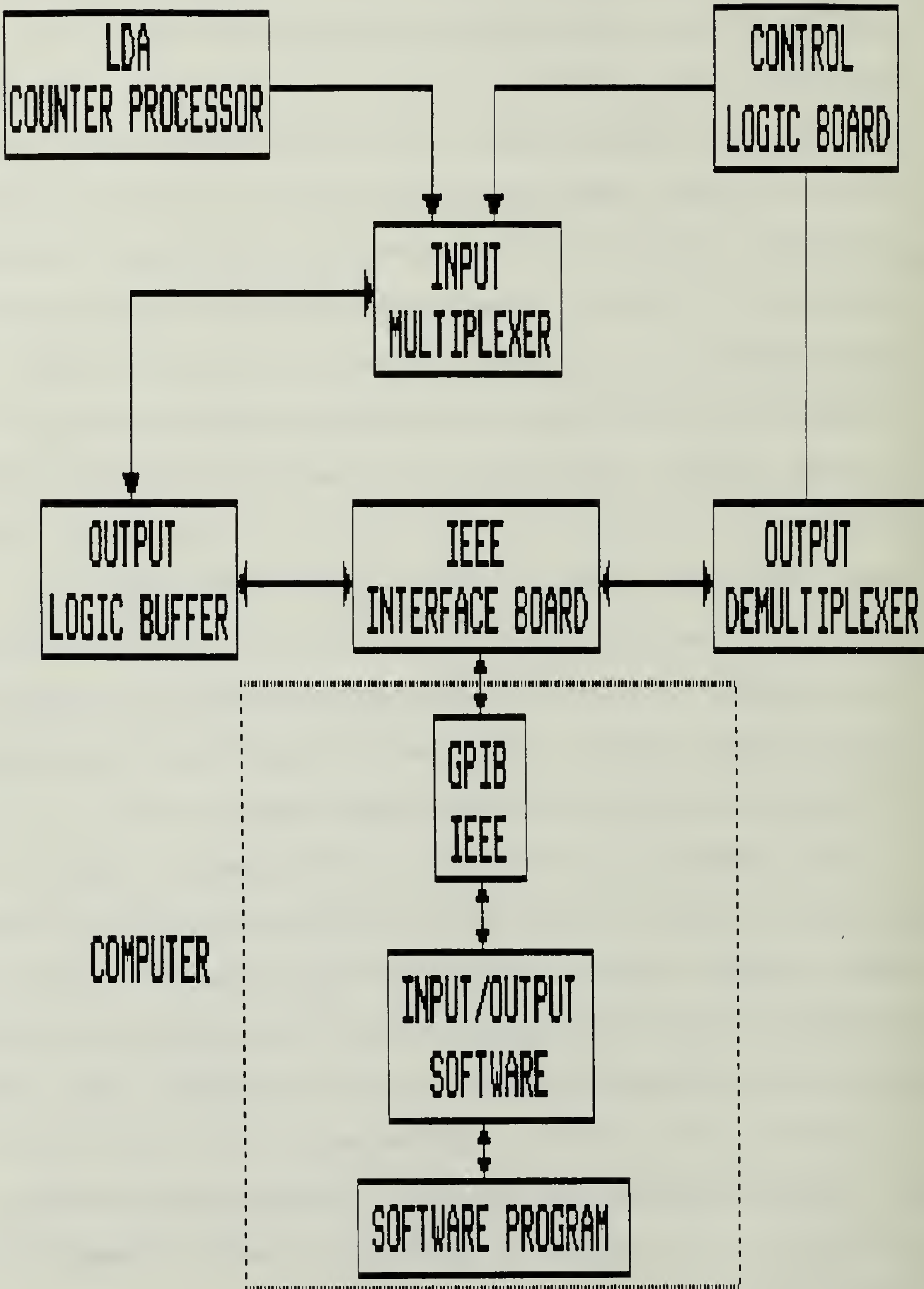

Figure 13 Binary Coded Data Flow

F. EQUIPMENT SET UP

Three separate equipment configurations were utilized to validate the system. First utilized was the calibration equipment setup, then the free jet and seeding apparatus and finally the wind tunnel setup.

The calibration setup is illustrated in Figure 14. Two different motors where used to drive the rotating wheel. A D.C. motor which could be varied from zero to about 2500 rpm and an A.C. motor which rotated at a constant velocity.

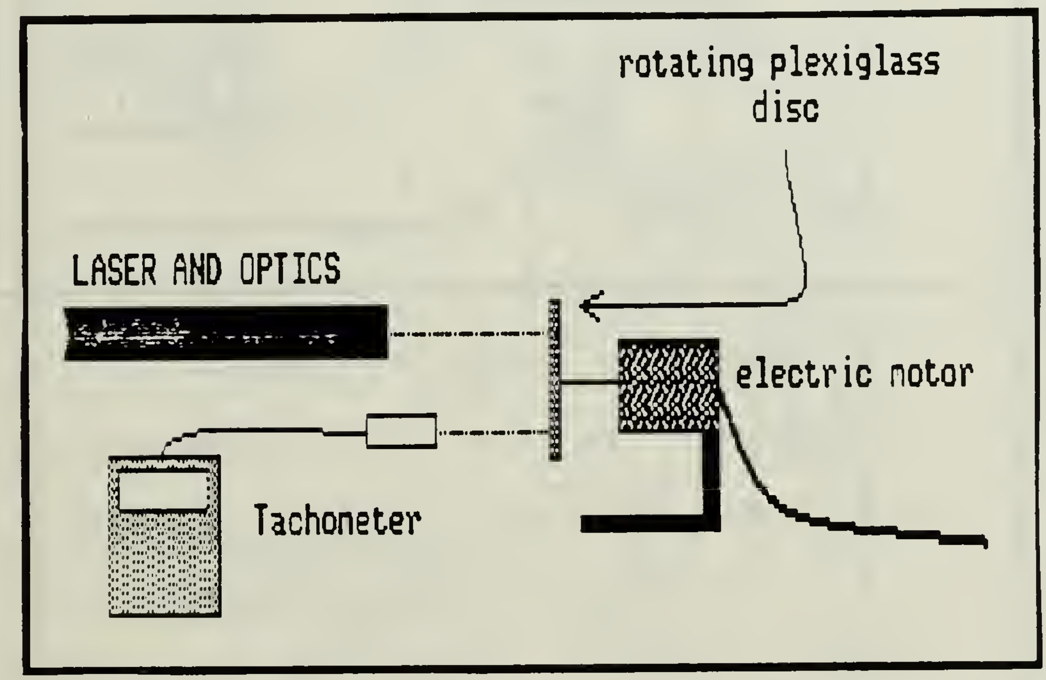

Figure 14 Calibration Setup

The apparatus used to achieve the free jet profile is illustrated in Figure 15. The free jet is a straight tube with a 14mm exit diameter. The seeding was fed into the nozzle via the venturi and aided by positive air pressure from the seeding canister. The seeding material used in this apparatus and also in the wind tunnel was a liquid aerosol of di(2-ethylhexyl)-phthalate or DOP. The seeding apparatus aerates the aerosol via a plastic tube perforated

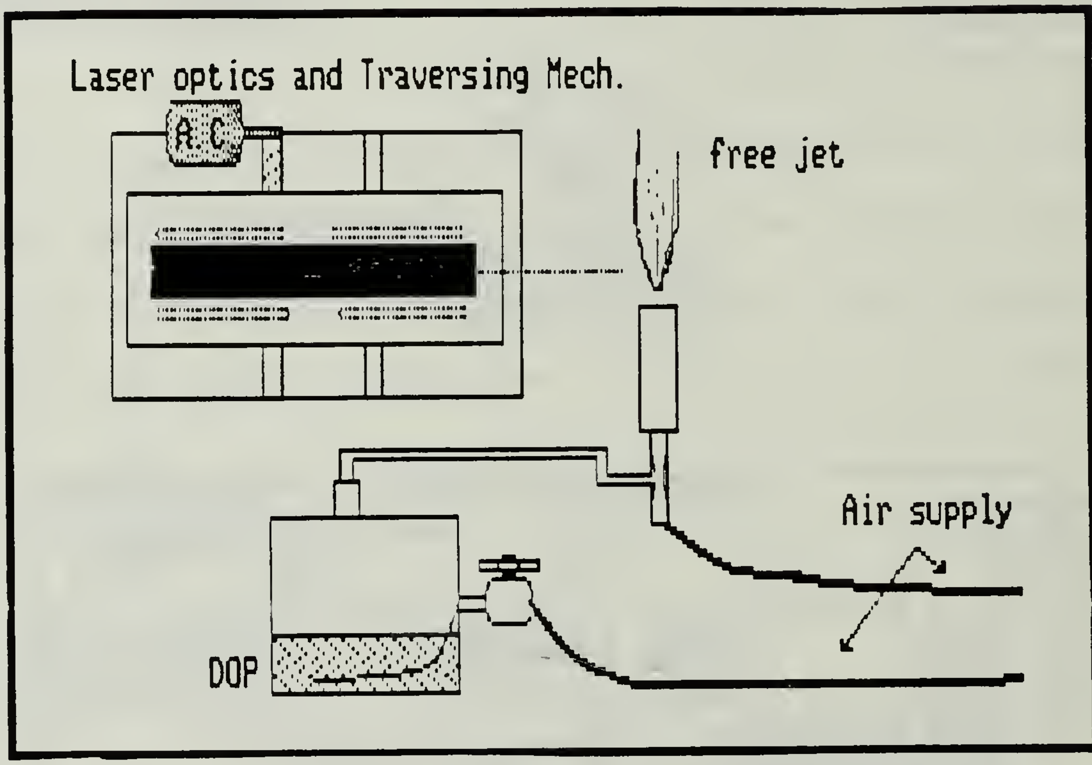

Figure 15 Free Jet Setup

with small pin-holes. In similar arrangements used for flow visualization the vaporized particles generated by the aerator are passed through a tube connected to a jet impactor. Particle sizes after the jet impactor are typically less than 1.3um when supply air pressure is at 25 psig [Ref 3 p. 1]. The device as outlined for this setup provided a better quality signal for the low powers of the He-Ne laser than did the jet impactor configuration.

Figure 16 illustrates the LDV setup as it was configured in orientation to the NPS low speed wind tunnel. The stainless steel tube was connected to the identical

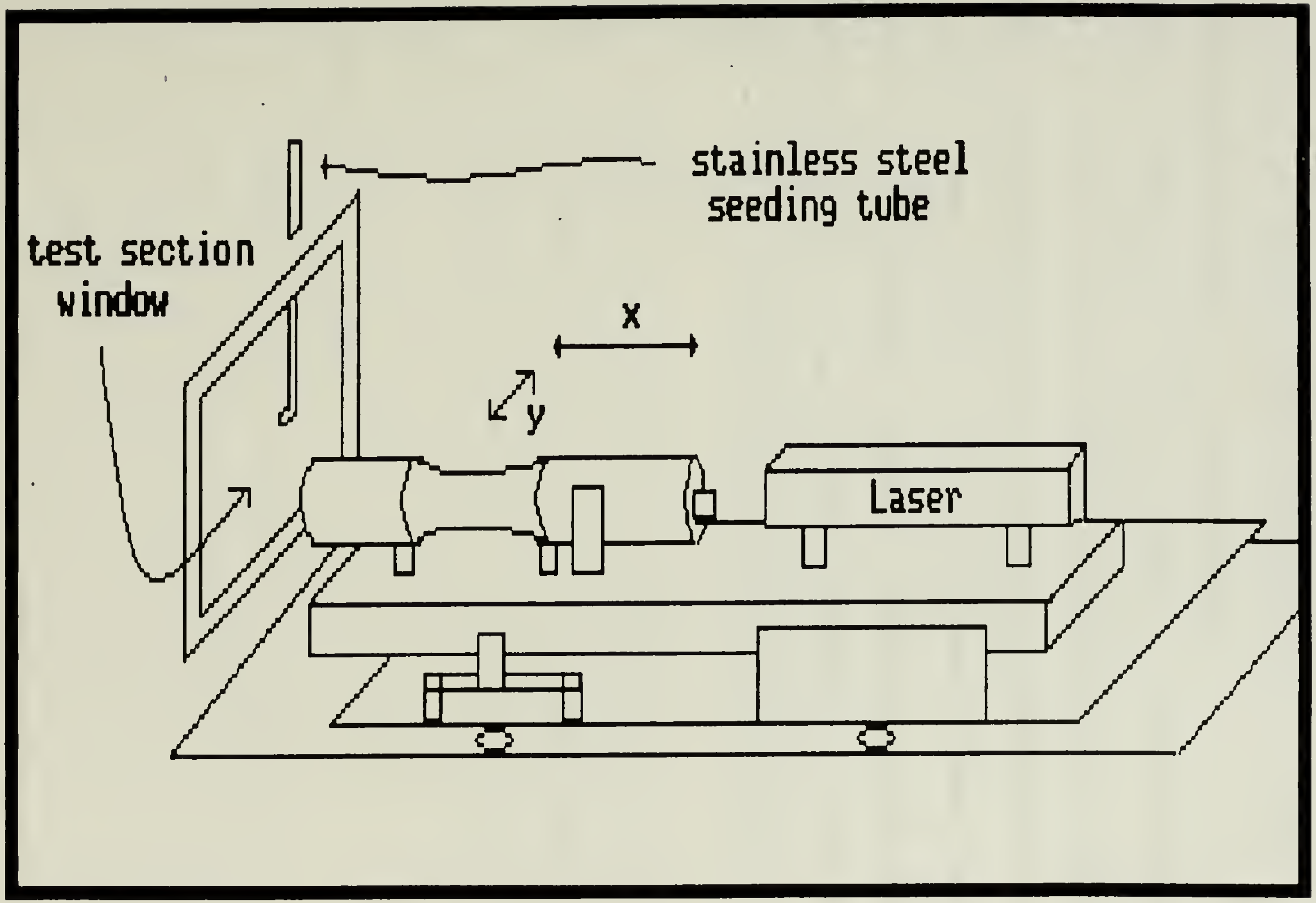

Figure 16 LDV - Tunnel Orientation

seeding generator used in the free jet apparatus. A full description of the physical dimensions and characteristic of the tunnel can be found in Reference 4.

The traverse mechanism constructed utilized two linear potentiometers, with digital readout provided, to accurately position the probe volume. Two A.C. reversible motors where used to drive a worm gear and threaded rod to move the laser mounting table. These motors were adjusted via a push button control box. The table could be adjusted to allow for approximately 12 inches of travel in both the x and y axis as labeled on the figure.

IV. DATA ACQUISITION

A. COMPUTER SOFTWARE

Dantec LDA2D computer software was used to interface the computer with the signal processing equipment. The software allows the user to specify the number of samples taken, the wave length of the laser beam, the beam separation, lens focal length, number of counters, and coincidence filter timing. The software provides for the establishment of a velocity window to further control data rejection.

The software calculates the velocity by use of the equations explained earlier. It also calculates velocity moments and produces graphical output of the resultant calculations.

B. CALIBRATION PROCEDURE

The D.C. motor was used first in order to verify the rpm of the wheel and thereby establish the calibration of the signal processing equipment over a range of velocities. The rpm of the wheel was varied from 0 to 2500 rpm and two readings were taken at each rpm setting. The LDV was set to obtain 1000 samples as each rpm setting stabilized. The mean velocity computed by the computer software was used to compare the results achieved. The comparative accuracy was set at 1.5% and the percent validation indicated values in excess of 900. The procedure was repeated several times to obtain an overall average. The procedure was also repeated using the A.C. motor which rotated at a stable rpm corresponding to 4.7 m/s.

C. FREE JET

To obtain the free jet profile measurements, the traversing system was manually positioned in 2mm increments across the 14 mm jet at 1/2 diameter away from the free jet exit. The measurements were made in laboratory coordinates from 2 to 16mm across the flow. Which was just at the edge of the free jet exit plane. The LDV was set to obtain 1000 samples with the comparative accuracy set at 1.5% and the percent validation indicating values in excess of 800. A 310mm focal lens was used to reduce power losses by reducing the transmission distance of the back scattered signal.

D. WIND TUNNEL DATA

The wind tunnel measurements were performed at velocities from 16 m/s to approximately 50 m/s. At a single stationary position in the free stream flow of the tunnel. The LDV and comparative accuracy settings were as before. The percent validation values indicated were in excess of 700. An existing data acquisition station was implemented to compare the results obtained in addition to standard pitot static probe.

V. RESULTS AND DISCUSSION

A. CALIBRATION RESULTS

Table 1 lists sample data obtained from the D.C. motor. The samples presented are averages of the total data taken. Due to radical fluctuations in the power supplying the D.C. motor the rpm, once established was extremely unstable. This required that the rpm readings from the tachometer be averaged over a 10 second period. The LDV, however obtained the 1000 samples in less than 5 seconds. This could account for the differences between the LDV and the tachometer values. Still the averaged error calculated using this technique was .67%.

TABLE 1 CALIBRATION DATA

RPM (TACH)	WHEEL VEL (M/S)	LDV VEL (M/S)
460	1.84	1.82
460	1.84	1.83
600	2.39	2.42
905	3.61	3.61
1340	5.35	5.36
1350	5.39	5.38
1830	7.30	7.31
1830	7.30	7.32
2300	9.18	9.24
2400	9.58	9.4
2500	9.97	10.06
2500	9.97	10.12

Using the A.C. motor which rotated at stable 4.7 m/s removed the requirement to time average the tachometer display. The error in Tachometer vs LDV measurements calculated using this motor was .01%.

For convenience the A.C. motor was used whenever beam alignment was adjusted and again before each test run in the free jet and tunnel. This was done in order to verify system performance.

B. FREE JET PROFILE

The velocity profile measured in the free jet is shown in Figure 17. It can be seen that the profile is not fully flat. However, the variations in the velocity from the centerline to the outside is approximately 8%. Part of the reasons for this is the somewhat non-uniform seed introduced to make measurements. The gradual falling of the velocity at the edges, unlike the sharp fall expected of a top-hat profile at the exit plane of a jet, is due to the development of the boundary layer along the nozzle walls.

Similar conclusions can be drawn for the turbulence intensity distribution also (see Figure 18). In the potential core of the jet, the turbulence intensity is low at the outer edges, it is fairly high approximately 28%. It should be noted that making measurements in this region of a jet is somewhat difficult unless the ambient flow is

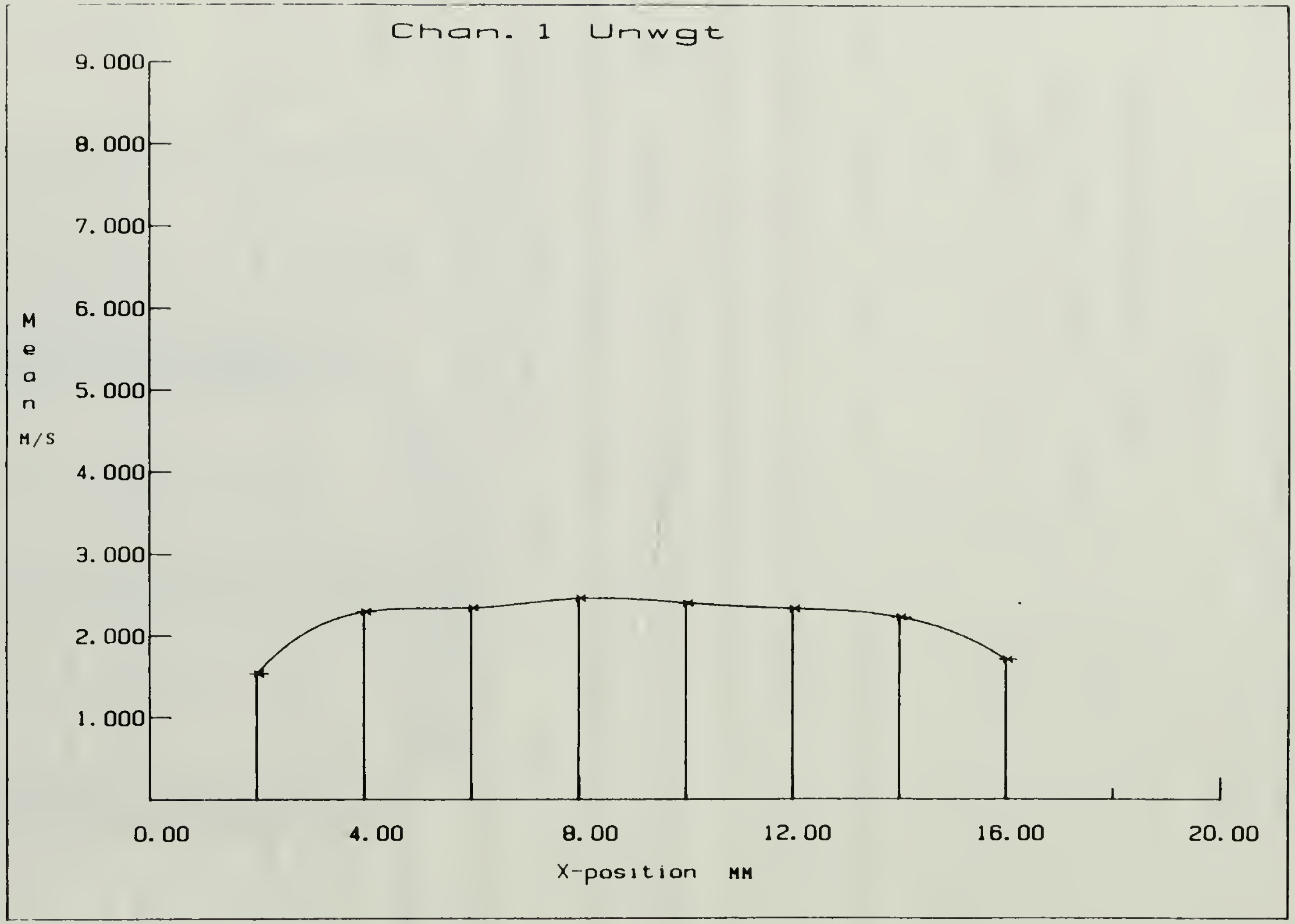

Figure 17 Free Jet Mean Velocity Profile

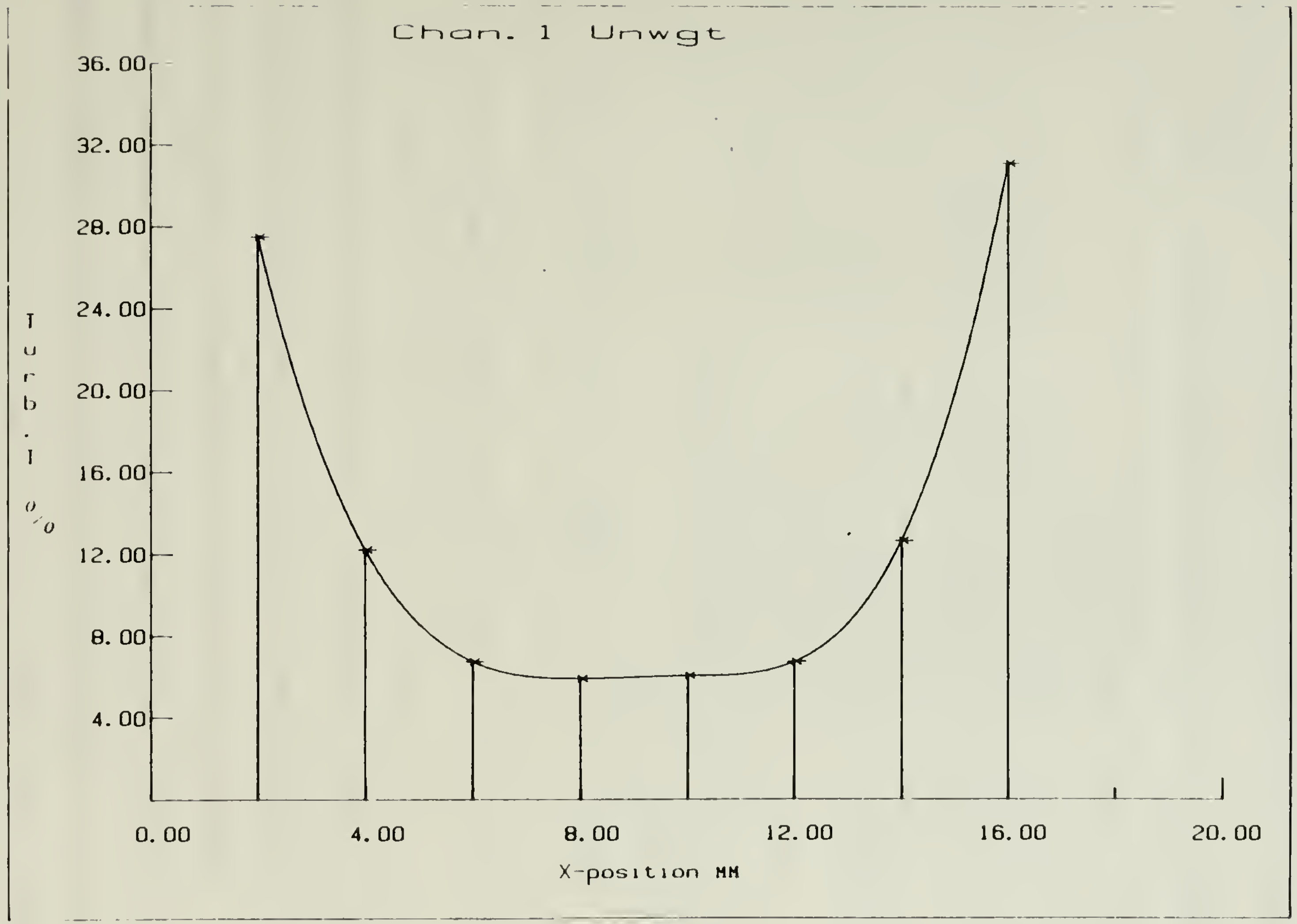

Figure 18 Free Jet Turbulence Intensity

also properly seeded, which was not the case in this experiment.

Some imperfections in machining the nozzle would also contribute to the effects discussed above.

C. WIND TUNNEL MEASUREMENTS

The wind tunnel velocity measurements compared extremely well with velocities simultaneously calculated by an existing data acquisition system. To determine velocity in the tunnel the existing system software program utilized delta-P, temperature, pressure, and established wind tunnel corrections in the following formulas:

[deltaP/q] = .93

q = 1.075 * deltaP (cmH2O) * 2.047 (psf/cmH2O)

$$\text{Velocity} = \text{sqrt}\left[\frac{2Q * 1715 * \text{Tunnel Temp}}{\text{Pstatic(psi)} * 144 * .9902}\right]$$

Delta-P was obtained from static ports positioned in the wind tunnel test section and the settling chamber (see Ref 5). The LDV velocity measurements were also compared against a pitot static system using the same program but utilizing the head pressure and static pressure ports on the pitot tube as the pressure inputs.

The velocities measured by the LDV were within 1% of the wind tunnel static port obtained results. A better comparison was realized in utilizing the pitot tube. The data in this case was within .1% of the pitot tube results.

VI. CONCLUSIONS AND RECOMMENDATIONS

A computer based laser doppler velocity system has been established in the Naval Postgraduate School low speed wind tunnel. The system is suitable for advanced classroom laboratories in the measurements of steady flow fields. The system can operate as a sole collection unit or can be used in conjunction with other data collection systems currently installed on the wind tunnel.

For purposes of instruction, the proper signal conditioning and seeding techniques can be illustrated and velocities obtained from a free jet flow. As an additional demonstration velocity measurements can be made in the wind tunnel.

The modular optics system is compatible with both the Argon-Ion laser and the He-Ne laser. The Argon-Ion laser should be utilized for purposes of research as it produces powers of about 4 watts. This would provide the higher signal levels needed to make measurements of the turbulence quantities at the large stand off distances necessitated by the test section dimensions. It is also suggested that the system be expanded to measure two velocity components simultaneously. The traversing mechanism should also be upgraded to provide a motor drive to control the vertical positioning of the probe volume. Eventually the entire mechanism should be integrated into the computer work station to optimize efficiency.

LIST OF REFERENCES

1. Durst, F., Principles and Practices of Laser-Doppler Anemometry, 2nd ed., Academic Press, 1981.

2. NASA Contractor Report 177386, Laser Doppler Velocimetry Primer, by William D. Bachalo, December 1985.

3. O.M. Griffin and M.D.Kelleher, The Generation Of Liquid Aerosols For The Visualization Of Oscillatory Flows, International Congress on Instrumentation In Aerospace Simulation Facilities, 5th, 1973.

4. Laboratory Manual for Low Speed Wind Tunnel Testing, Department of Aeronautics, Naval Postgraduate School, October 1983.

5. J.A. DiMiceli, Computer-Controlled Data Aquisition And Analysis, Masters Thesis, Naval Postgraduate School, Monterey, California, September 1986.

INITIAL DISTRIBUTION LIST

		NO. COPIES
1.	Defense Technical Information Center Cameron Station Alexandria, Virginia 22304-6145	2
2.	Library, Code 0142 Naval Postgraduate School Monterey, California 93943-5000	2
3.	Satya Bodapati, Code 67 Bu Department of Aeronautics Naval Postgraduate School Monterey, California 93943-5000	10
4.	M. F. Platzer, Chairman Department of Aeronautics Naval Postgraduate School Monterey, California 93943-5000	1
5.	Ricky E. Wilson 11496 115th N.W. Street Oak Harbor, Washington 98277	5
6.	Jack King Department of Aeronautics , Code 67JK Naval Postgraduate School Monterey, California 93943-5000	1
7.	D. P. Bencze Chief, Applied Aerodynamics Branch NASA Ames Research Center (M. S. 227-6) Moffett Field, California 94035	1
8.	Chief, Fluid Mechanics Laboratory NASA Ames Research Center (M. S. 260-1) Moffett Field, California 94035	1
9.	Dr. M. S. Chandrasekhara NASA Ames Research Center (M. S. 260-1) Moffett Field, California 94035	1

10. Engineering Sciences Divison 1
Attn: T. L. Doligalski,
Chief, Fluid Dynamics
U.S. Army Research Office
P. O. Box 12211
Research Triangle Park
North Carolina 27709-2211

11. Directorate of Aerospace Sciences 1
Attn: Hank E. Helin, Program Manager
AFOSR/NA
Bolling Air Force Base
Washington, DC 20332-6448

12. Naval Air Systems Command 1
Attn: Harry Berman, Program Manager
AIR-931k
Washington, D.C. 20361-9320

13. Office of Naval Research 1
Attn: Spiro Lekoudis, Program Manager
Code 1132F
800 North Quincy Street
Arlington, Virginia 22217-5000

14. David Taylor, NSRDC, Code 8 1
Attn: Jim Nichols
Aviation and Surface Effects Department
Bethesda, Maryland 20084

Thesis
W6433 Wilson
c.1 Steady flow field measurements using Laser Doppler Velocimetry.